

PHASE ORDERING DYNAMICS OF COSMOLOGICAL
MODELSJ. A. N. Filipe¹ and A. J. BrayDepartment of Theoretical Physics
The University, Manchester M13 9PL, United Kingdom

ABSTRACT

The ordering dynamics of the Higgs field is studied, using techniques inspired by the study of phase ordering in condensed matter physics, as a first step to understanding the evolution of cosmic structure through the formation of topological defects in the early universe. The common feature of these different physical processes is scaling. A fully analytical approximate scheme to the linear-gaussian approach is proposed to evaluate 1-point, 2-point, etc. scaling functions for the ordering dynamics of the $O(n)$ -symmetric Higgs-field models.

PACS: 64.60.Cn, 64.60.My, 98.80.Cq

¹Present address: BioSS, The University of Edinburgh, James Clerk Maxwell Building, The King's Buildings, Edinburgh EH9 3JZ, United Kingdom

I. INTRODUCTION

When a system is rapidly quenched from a disordered phase of high symmetry to a multiphase region of lower symmetry it undergoes a spontaneous symmetry breaking (SSB) phase transition. During this transition the system develops a spatial structure of randomly distributed domains which grow with time. This phase ordering process has been extensively studied in the context of condensed matter systems [1], especially those with a non-conserved order parameter (model A) [2], described by the time-dependent Ginzburg-Landau (TDGL) equation. There is much evidence that in the late stages of growth these systems enter a scaling regime [3], in which the two-point correlation function has the scaling form

$$C(r; t_1; t_2) \stackrel{D}{\sim} \langle \tilde{\phi}(\mathbf{x}; t_1) \tilde{\phi}(\mathbf{x} + \mathbf{r}; t_2) \rangle \stackrel{E}{=} f\left(\frac{r}{L(t_1)}; \frac{L(t_2)}{L(t_1)}\right); \quad (1)$$

where $\tilde{\phi}$ is the vector order parameter field, $L(t)$ is the characteristic length scale at time t after the quench, f is a scaling function, and angled brackets indicate an average over initial conditions (and thermal noise, if present).

A similar kind of phase-ordering phenomenon is believed to have occurred in the early universe. While the big-bang theory has been widely verified by observations (confirming that the universe began in a very hot, dense state and has expanded and cooled down ever since [4]), the origin of cosmic structure remains unexplained. According to the isotropy of the microwave background radiation (left over from the early matter-radiation decoupling transition) the early matter distribution was very uniform. How did the universe evolve from its primordial smooth state to its present state of lumpiness, where matter concentrates in galaxies and galaxy clusters [5] forming a very-large scale structure? It is believed that tiny large-scale density fluctuations, present at decoupling, could, if strong enough, have resisted the overall expansion and grown under gravitational collapse. Matter in the overly dense regions of space would have clumped together to produce general structure. What was the origin of these small fluctuations, however, and how could they have generated the kind of large-scale structure we see today? Based on a process central to unified theories of particle physics—that as the early universe cooled down a hypothetical field, the Higgs field, underwent a SSB transition—it has been suggested [6] that the consequent field ordering and defect formation could have provided the mechanism to generate structure. Field defects would form unavoidably, because ‘vacuum’ configurations above the horizon scale are uncorrelated. Since the defects carry energy they could provide the fluctuations around which matter would aggregate [5, 7, 8].

The purpose of this paper, is to use some of the techniques developed in the framework of model A’ dynamics (i.e. the TDGL equation) to study the Higgs

model ordering kinetics. This problem is technically more difficult than model A because the equation of motion describes a damped wave propagation rather than a purely dissipative process. However, these non-conserved field ordering processes are likely to exhibit similarities at late times, where a scaling regime is expected to occur [9, 10, 11]. A difference, though, is that here the characteristic length scale grows linearly with time, $L(t) \propto t$, while $L(t) \propto t^{1/2}$ for model A.

While domain growth phenomena, governed by the kinetics of topological defects, have been fairly well understood within model A dynamics, a first principles calculation of the scaling functions has proved to be a most difficult task, and various closed-approximation schemes to evaluate the scaling function $f(x; q)$ of equation (1) have been proposed in the past few years [12, 14]. The key technique, exploited by several authors [12]–[16], is to introduce a mapping $\tilde{\phi}(r; t) = \tilde{\phi}(\mathbf{r}; t)$ between the order parameter field and an auxiliary field $\mathbf{r}(r; t)$ which has, near a defect, the physical interpretation of a position vector relative to the defect. With this new variable, the problem of describing the field at each instant of time is transformed into a problem of describing the evolution and statistics of the defect network. This approach enables the use of a physically plausible and mathematically convenient gaussian distribution for \mathbf{r} . Such a distribution is unacceptable for the order parameter itself, since this is effectively discontinuous at the domain size scale. The application of this sort of approach to the scalar-field model A has recently received a critical review by Yeung et al. [17]. Methods based on a description of the wall dynamics lead to an approximate linear equation for $\mathbf{r}(r; t)$, or for its correlator $\langle \mathbf{r}(x; t_1) \mathbf{r}(x + \mathbf{r}; t_2) \rangle$. A different and promising approach, due to Mazonko [14], aims at deriving a closed non-linear equation for $C(\mathbf{r}; t_1, t_2)$, built on the equation of motion for the scalar-field model A, and the assumption that the field \mathbf{r} is gaussian distributed at all times. It has the virtue of yielding results with a non-trivial dependence on the spatial dimension d and it is also easily extensible to $O(n)$ -component systems. Despite the uncontrolled nature of the gaussian assumption these approaches have been shown to give good results, displaying most of the expected physical features [14, 16]. For the nonconserved dissipative dynamics of model A, it has been argued that the gaussian approximation becomes exact in the limit of large spatial dimension d , while for fixed d it provides the starting point for a systematic treatment [18]. It is also correct for any d in the limit of large n . For the Higgs field model considered here, the gaussian approximation is again exact for large n , but the large- d limit does not seem to be simple. Nevertheless, by incorporating topological defects in a natural way, the gaussian field approach provides the simplest non-trivial approximation scheme for the dynamics of phase ordering.

In section 3 we attempt to apply the Mazenko approach to the $O(n)$ -field Higgs model. The late-time pair correlation function is then given by the Bray-Puri-Toyoki (BPT) function (20) [15], as a function $C(\mathbf{r}; n)$ of the normalized correlator of ϕ , $\langle \phi(\mathbf{r}; t_1; t_2) \rangle$, which obeys an approximate non-linear equation. The BPT function embodies the asymptotic defect structure, while $\langle \phi(\mathbf{r}; t_1; t_2) \rangle$ describes the dynamical dependence of $C(\mathbf{r}; t_1; t_2)$. The mapping used by Mazenko [14, 16], however, restricts the field to evolve within the bound $|\tilde{\mathbf{j}}| \leq 1$, which is incompatible with the oscillatory bulk relaxation of the Higgs field, and leads to an inconsistent approach. The difficulties with this approach, however, motivate our next attempt to tackle the problem. In section 4 we consistently eliminate the field bulk oscillations by restricting the asymptotic field dynamics to the ‘vacuum manifold’. Extending Mazenko’s gaussian approach to the Non-Linear Sigma Model (NLSM), using the unit vector mapping $\tilde{\mathbf{r}} = \phi = \mathbf{j}/|\mathbf{j}|$, the pair correlation function is still given by the BPT function, but now ϕ obeys a different approximate equation. Rather than solving numerically this equation for ϕ , which is rather complicated, in section 5 we propose a fully analytical approximate scheme to evaluate C . This amounts to replacing ϕ by its large- n limit in the argument of the BPT function, but keeping the remaining n -dependence unchanged. As $n \rightarrow \infty$ the equation for ϕ becomes linear and exactly solvable [9], so we may call this scheme the Linear-Gaussian (LG) approach. Although we cannot use the NLSM for a scalar field, the approach still holds for this case if one takes $n = 1$ in the BPT function. In section 6 the LG approach will be generalized to evaluate other kinds of scaling functions, such as the average of the energy density and its correlation function.

II. THE HIGGS FIELD MODEL

In this section we briefly review basic notions about the cosmological background model. The Higgs field model is presented and its dynamics are discussed.

As is usual practice, we shall consider a flat expanding universe as the model for the bulk cosmological background [4, 5]. In this case the local curvature is zero and the metric is space-independent, given by

$$ds^2 = c^2 dt^2 - a(t)^2 d\mathbf{r}^2 = a(\eta)^2 c^2 d\eta^2 - d\mathbf{r}^2; \quad (2)$$

where: t and \mathbf{r} are comoving coordinates (i.e. the reference frame is moving with the cosmic flow); $a(t)$, or $a(\eta)$, is the space expansion factor; η , the conformal time, defined by

$$d\eta = dt/a(t); \quad (3)$$

plays the role of ‘real time’ in a static universe: the horizon of an ‘event’ after a time t – its maximum range of influence after time t – is given by $h(t) = \int_0^{R_h} d\mathbf{r} =$

$\int_0^R c dt = a(t) = c_0 \int_0^R d = c(t)$. In a flat universe, the function

$$() = 2 \frac{d \ln a(t)}{d \ln t}; \quad (4)$$

varies slowly with time from $= 2$ (radiation era) to $= 4$ (matter era). Away from the matter-radiation decoupling transition ϵ can be regarded as a constant and the expansion factor is given by a power-law $a(t) = a_0 t^{(1/3)}$ [5, 9].

In the early radiation dominated era the energy was dominated by relativistic particles (with equation of state $p = \epsilon/3$), yielding a $\epsilon \propto t^{-2}$ and $a \propto t^{1/2}$. Here p and ϵ are the uniform background pressure and energy density. Once the universe cooled down and matter decoupled from radiation this became the dominant source of gravitation (with negligible pressure $p \approx 0$), yielding a $\epsilon \propto t^{-3}$ and $a \propto t^{2/3}$ in the matter dominated era. As matter became transparent to radiation, the matter perturbations started to grow.

A simple class of SSB theories is provided by the (real) n -component Higgs field models, where a global $O(n)$ symmetry is broken [5, 9, 11]. These theories include several cases where topological defects form: domain walls ($n = 1$), global strings ($n = 2$), global monopoles ($n = 3$) and global textures ($n = 4$), which are of potential interest as a mechanism to generate cosmic structure.

The dynamics of the Higgs field $\tilde{\phi}(r;t) = (\phi^1; \dots; \phi^n)$ in an expanding universe is derived from the Lagrangian density [5]

$$L(r;t) = \frac{1}{2} \partial_\mu \tilde{\phi} \partial^\mu \tilde{\phi} - \frac{1}{2} \dot{\tilde{\phi}}^2 - a^2(t) V(\tilde{\phi}); \quad (5)$$

where r is with respect to comoving coordinates, and $V(\tilde{\phi})$ is a generalized 'double-well' potential with an $O(n)$ symmetric 'vacuum manifold' where $\tilde{\phi}^2 = 1$. Minimizing the action $S = \int dt \int d^3r a(t)^3 L(r;t)$ (where $dt d^3r a(t)^3$ is the covariant 4-volume element) with respect to variations of $\tilde{\phi}$, and using conformal time, yields the equation of motion

$$\frac{\partial^2 \tilde{\phi}}{\partial \eta^2} + \frac{\partial \tilde{\phi}}{\partial \eta} = -r^2 \tilde{\phi} - a(\eta)^2 \frac{\partial V}{\partial \tilde{\phi}}; \quad (6)$$

a wave equation with a damped 'friction force' ($= \partial \tilde{\phi} / \partial \eta$), which minimizes expansion in the comoving frame (and destroys the Lorentz invariance), and a non-linear force $\partial V / \partial \tilde{\phi}$ which drives the field to the 'vacuum manifold'. The initial conditions

corresponding to a disordered state before the SSB phase transition shall be discussed in the appendix, where we present the solution of (6) in the limit $n \rightarrow 1$. The price for using conformal time is to have an effective potential in equation (6) with a time-dependent amplitude. The particular form of the potential, however, should not affect in any essential way the late-time dynamics and scaling properties.

We expect, for instance, the main effect of $a(t)^2$ to be a decrease by a factor $1/a$ in the comoving size of the defects core, which simply speeds up the system entry into the scaling regime. To simplify the subsequent discussion we shall from now on discard the a^2 factor in the equation of motion (6). We will not really need that for computational purposes, as we shall be using the NLSM.

Taking conformal time on the same footing as real time, equation (6) can be viewed as a 'general-relativistic analogue' of the TDGL equation, describing the dynamics of non-conserved systems. The Higgs Hamiltonian density corresponding to (5)

$$H(\mathbf{r};t) = \frac{1}{a(t)^2} \left[\frac{1}{2} (\partial_\mu \tilde{\phi})^2 + \frac{1}{2} |\dot{\tilde{\phi}}|^2 + V(\tilde{\phi}) \right]; \quad (7)$$

is (apart from $1/a^2$) similar to that of a static (Minkowski) universe, and compared to the TDGL model has an extra 'centripetal' term $(\partial_\mu \tilde{\phi})^2$. For a vector field in the 'vacuum manifold' it leads to an energy density which decays (due to expansion and dissipation) like the background, $1/t^2$. Therefore, the Higgs field yields density fluctuations of constant amplitude $\delta\rho/\rho = (\delta\tilde{\phi}/\tilde{\phi}) = \text{const}$ which, through Einstein's equations, provide a source for perturbations in the matter distribution.

Assuming the existence of a late-time scaling regime (which has been confirmed by numerical simulations [9, 10, 11]), the dimensional analysis of (6) leads to a characteristic scale growing with the horizon

$$L(t) \propto c; \quad (8)$$

implying that the field defects move with relativistic speed. We therefore expect the pair correlation function (1) to take the asymptotic scaling form $C(\mathbf{r}; t_1; t_2) = f(\mathbf{x}; q)$, with scaling variables $\mathbf{x} = \mathbf{r}/c_1$ and $q = c_2/c_1$, where $\mathbf{r} = |\mathbf{r}_1 - \mathbf{r}_2|$ is the distance between the two points.

Causality constrains the field correlations after the SSB transition. Two field configurations at times t_1 and t_2 can only be causally correlated if their distance r is below the sum of their horizons c_1 and c_2 (i.e. if the horizons intersect). Therefore, the condition for $C(\mathbf{r}; t_1; t_2) \neq 0$ is (taking $c = 1$)

$$r < c_1 + c_2; \quad (9)$$

If one of the horizons contains the other configuration (c_1 or $c_2 > r$) the correlations are 'direct'. Otherwise, 'indirect' correlations can occur through common causal correlations with intermediate points in the region of intersection of the horizons.

Unlike purely relaxing systems, the wave nature of the Higgs dynamics forces the late-time saturating field not to satisfy $\tilde{\phi} \sim 1$ even if its initial condition does. To see how the field tends to its 'vacuum manifold' we linearize equation (6) as $\tilde{\phi} \sim$

approaches a given 'vacuum' state $\tilde{\phi}_0$. Considering a single-domain region where $\tilde{\phi}$ can be taken as uniform, and noticing that the only restoring force is parallel to $\tilde{\phi}_0$ (normal to the manifold) due to the symmetry of the 'vacuum', we find, at late-times

$$\tilde{\phi}(\mathbf{r}) = \tilde{\phi}_0 + \frac{1}{a(\mathbf{r})} [c_1(\mathbf{r}) \cos(A(\mathbf{r})) + c_2(\mathbf{r}) \sin(A(\mathbf{r}))]; \quad (10)$$

where $A^2 = -\partial^2 V / \partial (\tilde{\phi}^2)$, and $c_1(\mathbf{r})$ and $c_2(\mathbf{r})$ are arbitrary constants. For a scalar field $\tilde{\phi}(\mathbf{r}) = \tilde{\phi}_0$ is replaced by $j(\mathbf{r})$. We conclude that the Higgs field saturates with damped oscillations.

III. GAUSSIAN THEORY FOR A 'SOFT' FIELD

In this section we apply to the Higgs model the gaussian approach proposed by Mazenko [14] for the TDGL dynamics. Although the approach, which is based on an unphysical mapping for the Higgs dynamics, leads to an inconsistent theory, it will motivate the implementation of a gaussian approach for a unit vector field in section 4.

To derive an equation for the pair correlation function (1), we multiply the equation of motion (6), evaluated at point (1) $(\mathbf{r}_1; t_1)$, by $\tilde{\phi}(\mathbf{r}_2; t_2)$ and average over the ensemble of initial conditions, yielding the exact equation

$$C(\mathbf{r}_1; \mathbf{r}_2) + \frac{1}{r_m^2} C(\mathbf{r}_1; \mathbf{r}_2) = r_m^2 C(\mathbf{r}_1; \mathbf{r}_2) + F(\mathbf{r}_1; \mathbf{r}_2); \quad (11)$$

where the driving force, or non-linear (NL) term, is

$$F(\mathbf{r}_1; \mathbf{r}_2) = \langle \tilde{\phi}(\mathbf{r}_2) \frac{\partial V}{\partial \tilde{\phi}(\mathbf{r}_1)} \rangle; \quad (12)$$

and $C(\mathbf{r}_1; \mathbf{r}_2) = \langle C(\mathbf{r}_1; \mathbf{r}_2) \rangle = \langle \tilde{\phi}(\mathbf{r}_1) \tilde{\phi}(\mathbf{r}_2) \rangle$, etc. To transform (11) into a closed equation we need to write the NL term as some approximate non-linear function of $C(\mathbf{r}_1; \mathbf{r}_2)$. A key idea, exploited by several authors within the TDGL dynamics [12, 14, 16], is to employ a non-linear mapping between the order parameter $\tilde{\phi}(\mathbf{r}; t)$ and an auxiliary 'smooth' field $\mathbf{m}(\mathbf{r}; t)$. This new variable describes the late-time defect network structure, which will have formed at the late stages of field ordering, and allows for the approximation to be implemented. The most obvious way to define the function $\tilde{\phi}(\mathbf{m})$, is to follow Mazenko's suggestion [14] of using the equilibrium profile equation of an isolated defect (in a comoving frame)

$$r_m^2 \tilde{\phi} = \partial V / \partial \tilde{\phi}; \quad (13)$$

with boundary conditions $\tilde{\phi}(0) = 0$ and $\tilde{\phi}(\mathbf{m}) \rightarrow \tilde{\phi}_0$ as $|\mathbf{m}| \rightarrow \infty$, and where r_m is the gradient with respect to \mathbf{m} . Close enough to a defect (i.e. for $|\mathbf{m}| \ll L(\mathbf{r})$,

where the field is unaffected by neighboring defects) $\mathbf{m}(\mathbf{r}; \mathbf{j})$ can be identified as the comoving position vector of point \mathbf{r} from the (nearest part of the) defect. This picture requires, of course, that $n \rightarrow \infty$. With (13) the magnitude of $\tilde{\mathbf{m}}$ is a monotonically increasing function of the magnitude j , approaching for large j the 'attractor' value 1 imposed by the potential. For a scalar field, the function m has a typical sigmoid form.

The mapping (13) restricts the field magnitude to be $j \leq 1$. This is appropriate for diffusion fields evolving from a disordered state, but is physically incorrect for the Higgs field dynamics, where the system self-organizes oscillating about the 'vacuum' states, as shown by (10). While we can prove that the use of (13) leads to an inconsistent theory [19], it seems unlikely that an adequate one-to-one mapping could be defined for this problem. In section 4 we shall overcome this technical difficulty by restricting the field dynamics to the 'vacuum manifold', $\tilde{m}^2 = 1$. Meanwhile, for completeness we will pursue this approach a little further using (13) to derive a closed equation for $C(1;2)$.

Following Mazenko [14], we now assume that $\mathbf{m}(\mathbf{r}; \mathbf{j})$ is a gaussian random field (with zero mean) at all times, described by the pair distribution function

$$P(\mathbf{m}(1); \mathbf{m}(2)) = N^n \exp \left\{ -\frac{1}{2(1-\tilde{m}^2)} \left[\frac{\mathbf{m}(1)^2}{S_0(1)} + \frac{\mathbf{m}(2)^2}{S_0(2)} - \frac{2\mathbf{m}(1) \cdot \mathbf{m}(2)}{S_0(1)S_0(2)} \right] \right\}; \quad (14)$$

$$S_0(1) = \langle \mathbf{m}(1)^2 \rangle; \quad C_0(1;2) = \langle \mathbf{m}(1) \cdot \mathbf{m}(2) \rangle; \quad (15)$$

$$C(1;2) = \frac{C_0(1;2)}{S_0(1)S_0(2)}; \quad (16)$$

where $N = \frac{1}{2^{n/2} (1-\tilde{m}^2) S_0(1) S_0(2)}$, and $\mathbf{m}(1)$ and $\mathbf{m}(2)$ are the same (arbitrary) component of $\mathbf{m}(1)$ and $\mathbf{m}(2)$. All the averages over the ensemble of initial configurations are replaced by gaussian averages on \mathbf{m} , and can be evaluated as functions of the second moments $S_0(1)$, $S_0(2)$, and $C(1;2)$. However, from (8) and the mapping (13), according to which \mathbf{m} can be identified as a position vector, we anticipate the asymptotic scaling form

$$S_0(\mathbf{j}) = \frac{2}{L(\mathbf{j})^2}; \quad (17)$$

where L is a parameter to be determined. Thus, within a gaussian approach, the only variable in the problem is the function $C(1;2)$, which accounts for the particular dynamics of $\tilde{\mathbf{m}}$.

The driving force (12) in equation (11) is then given, as a non-linear function of $C(1;2)$, by Mazenko's result [14, 16]

$$F(1;2) = \frac{2}{\partial S_0(1)} \frac{\partial C(\mathbf{j})}{\partial \mathbf{j}} = \frac{C(\mathbf{j})}{2} \frac{\partial C(\mathbf{j})}{\partial \mathbf{j}}; \quad (18)$$

where $C = \langle \phi^2 \rangle$ and we have used (17). Note that, by use of the mapping (13), there is no longer any explicit dependence on the potential $V(\tilde{\phi})$ in (18), though the relation between $\tilde{\phi}$ and ϕ depends on V . At late times the field will be saturated almost everywhere except at the defect cores (whose size is much smaller than the domain scale), and we may, for simplicity, evaluate the gaussian averages replacing the problem mapping (13) by its discontinuous asymptotic form $\tilde{\phi}(\phi) = \phi = \text{sign}(\phi)$ for a vector field, or $\tilde{\phi}(\phi) = \text{sign}(\phi)$, for a scalar field. At late times, therefore, the detailed form of the potential is not important (although it must, of course, have the Mexican hat' form in order to support non-trivial solutions of (13)). This is in accord with the expected 'universal' nature of the late-stage scaling behavior.

Evaluating the pair correlation function $C(1;2)$, using (14) and the mapping above, yields the explicit relation $C = C(\phi; n)$, which we will call the BPT function' [15],

$$C(\phi) = \frac{\langle \phi(1) \phi(2) \rangle}{\langle \phi(1) \rangle \langle \phi(2) \rangle} \quad (19)$$

$$= (1;2) \frac{n}{2} B\left(\frac{n+1}{2}; \frac{1}{2}\right) F\left(\frac{1}{2}; \frac{1}{2}; \frac{n+2}{2}; (1;2)^2\right); \quad (20)$$

where $B(x;y)$ is the beta function and $F(a;b;c;z)$ is the hypergeometric function. The substitution of (18) and $C(\phi; n)$ into equation (11) yields the approximate closed equation for $(1;2)$, which for a vector field must be regarded as the independent variable. In the limit $n \rightarrow 1$ the BPT function reduces to $C(\phi; 1) = S_0$, yielding $F(1;2) = C(1;2) = S_0(1)$, and (11) becomes a linear equation.

We now focus on the pair correlation function at equal times ($t_1 = t_2 = t$), which is of interest by itself and also yields the initial condition to solve the general equation [16]. Equation (11) then reads

$$\frac{1}{2} C(1;2) = C(1;2) + \frac{1}{2} G(1;2) = r^2 C(1;2) + F(1;2); \quad (21)$$

where $G(1;2) = \langle \phi^2 \rangle$, etc. The unknown quantity $C(1;2)$ may be eliminated to get a third order equation in C . Then, replacing $F(1;2)$ by its approximate form (18), using (17), and looking for an isotropic scaling solution $C(r; \phi) = f(x)$, which implies $(r; \phi) = (x)$, with $x = r^{-1}$, leads to the equation for $f(x)$:

$$\frac{x(4-x^2)^n}{2} \omega + 3 \phi^0 \omega_D + \phi_D^0 + x^2 \frac{3(1-2)}{2} + 2(d+1) \phi^n \omega + \phi_D^0 \quad (22)$$

where $\phi^0 = d = dx$, etc, $D(\phi) = C = C$, $D(\phi) = C = C$, and $C = \langle \phi^2 \rangle$, etc. The NL functions $D(\phi)$ and $D(\phi)$ are obtained from (20) and embody all

the n -dependence of (22). The boundary conditions for equation (22) are $\phi(0) = 1$, from definition (15), $\phi'(0) = 0$, from $\phi(x) = 1 - O(x^2)$ as $x \rightarrow 0$, and $\phi(2) = 0$, from $C(x) \rightarrow 0$ as $x \rightarrow 0$ and the causal condition $f(x) = 0$ for $x > 2$. We notice that the boundary points are both singular, which makes the numerical solution of (22) difficult.

For a scalar field the BPT function (20) can be inverted to give $\phi = \sin(C/2)$, yielding a NL term $F(1;2) = (2 - S_0(1)) \tan(C(1;2)/2)$. Hence we can express (22) as an explicit non-linear equation for the scaling function $C(x; \epsilon) = f(x)$:

$$\begin{aligned} & \frac{x(4-x^2)}{2} f(x)^{(d)} + x^2 \frac{3(2)}{2} + 2(d+1) f(x)^{(d)} \\ & \frac{x}{2} (2)(2-3) + \frac{2}{x} (1)(d-1) f(x)^{(d)} \\ = & \frac{2}{(1)} \tan \frac{1}{2} f(x) + x \sec^2 \frac{1}{2} f(x) f^{(d)} : \end{aligned} \quad (23)$$

To perform a small- x expansion of (23), we recall that with the mapping $\phi = \sin(m)$, used to evaluate $C(x)$, the condition $f(0) = h^2 i = 1$ has been built into the theory (although in an inconsistent manner). We find that $f(x)$ admits a series in odd powers of x (implying that all derivatives at $x = 0$ are determined without recursion), giving the linear behaviour, or Porod's regime [21],

$$f(x) = 1 - \frac{1}{(d-1)(d-1)} x^2 + O(x^3) ; \quad (x \rightarrow 0) ; \quad (24)$$

which is a physical consequence of having 'sharp' walls at late times. To find the small- $(2-x)$ asymptotic form of $f(x)$, we notice that as $f(x) \rightarrow 0$ equation (23) becomes linear and has three independent solutions. Since the singularity at $x = 2$ is regular we try a Frobenius power series solution [20], $A_0(2-x)^p (1 + \sum_{k=1}^{\infty} a_k (2-x)^k)$, and find that the equation admits a leading power-decay $f(x) \sim (2-x)^p$ as $x \rightarrow 2$, where p can assume any of the values: $p = 0, p = 1$ or $p = \frac{1}{2} + (d-1)/2$. $p = 0$ must be excluded as being incompatible with the boundary conditions (it would imply $A_0 = 0$), and thus the solution has the general asymptotic form as $x \rightarrow 2$:

$$f(x) \sim A_0^{(1)} (2-x)^{-(d-1)/2} f_1 + O((2-x)^{-d/2}) + A_0^{(2)} (2-x)^{-(d-1)/2} f_1 + O((2-x)^{-d/2}) : \quad (25)$$

Since the BPT function (20) has the same behaviour $C(x; n) \sim (d-1)/2$ (and $D, D' \rightarrow 0$) as $x \rightarrow 0$ or $n \rightarrow 1$, to linear order in the regime $x \rightarrow 2$ and $f(x)$ equation (22) is n -independent and identical to its large- n limit. In the appendix we discuss the large- n limit of the NLSM (28) and find that $f_1(x) \sim (2-x)^{-(d-1)/2}$ as $x \rightarrow 2$, for $d = 3$. Therefore, for any value of n , and at least for short-ranged initial conditions, we expect the leading power-law decay

$$f(x) \sim (2-x)^{-(d-1)/2} ; \quad (x \rightarrow 2) : \quad (26)$$

Although we are not looking to solve equation (23), we describe how one in principle could do it. From (24) and (9), the boundary conditions are: $f(0) = 1$, $f'(0) = \frac{1}{2} = \frac{1}{2} \frac{d}{dx} f(1)$ and $f(2) = 0$. The parameter is numerically determined by imposing the coefficient of the dominant solution in (25) to vanish, $A_0^{(2)}(\epsilon) = 0$. In the large- n limit, where equation (11) becomes linear and the gaussian approach is exact, can be found analytically. Comparing (11) with the linear equation (36), which amounts to compare the limit of (18), $F_1(1;2) = \frac{1}{2} \frac{d}{dx} f(1)$, with $f(1)$ given by (37), yields

$$\frac{1}{2} = 2T_0 = 3(2 + 1) = 2 : \quad (27)$$

In conclusion, although the mapping (13) discards the field oscillations (10) and leads to an inconsistent theory [19], equation (22)–(23), despite its intrinsic incorrectness bears no obvious signs of inconsistency. A Porod's regime (24) is obtained as a consequence of the 'sharp' wall constraint $\phi(x) = \text{sign}(x)$ used to evaluate $C(\epsilon; n)$. We have shown that the manner in which $f(x)$ vanishes at $x = 2$, given by (26), is independent of n and exact.

IV. GAUSSIAN THEORY FOR THE NON-LINEAR SIGMA MODEL

In this section we study the dynamics of a vector Higgs field within the NLSM. By constraining the field to lie on the vacuum manifold, this model automatically avoids the technical difficulties associated with the asymptotic bulk oscillations noted in section 3. We develop a gaussian approach, analogous to that of section 3, and derive an approximate equation for $C(1;2)$.

Long after the SSB phase transition the driving potential V closely confines the Higgs field to the 'vacuum manifold' almost everywhere (except at the field defect cores). We have shown, however, that the wave nature of the dynamics leads to a field bulk saturation accompanied by slow decaying oscillations about the 'vacuum state', preventing us to define an adequate one-to-one mapping between $\tilde{\phi}$ and an auxiliary field \tilde{m} . The mapping (13), for instance, forces the field to obey $\tilde{\phi}^2 = 1$ at all times and yields an inconsistent approach. To overcome this technical problem, we notice that the oscillations (10) are unlikely to have a major effect on the late-time dynamics of the field defect network (and thus on the scaling properties), and may thus be consistently discarded by restricting the $O(n)$ field dynamics to the vacuum manifold. Replacing the vanishing driving force $\partial V = \partial \tilde{\phi}$ in (6) by a non-linear coupling term which constrains the length of the field, the field evolution is now described by the non-linear sigma model (NLSM) equation [9]:

$$\frac{\partial^2 \tilde{\phi}}{\partial t^2} + \frac{\partial \tilde{\phi}}{\partial t} = r^2 \tilde{\phi} + T(r; \epsilon) \tilde{\phi} ; \quad (28)$$

where $T(\mathbf{r}; \sim)$ is the free Lagrangian density in (5)

$$T(\mathbf{r}; \sim) = \frac{1}{2} \frac{\partial^2 \sim}{\partial t^2} - \frac{1}{2} \nabla^2 \sim = \frac{1}{2} \frac{\partial^2 \sim}{\partial t^2} - \frac{1}{2} \nabla^2 \sim : \quad (29)$$

As another advantage of using the NLSM, the ordering dynamics becomes independent of the details of the potential $V(\sim)$ and, in particular, the factor $a(\sim)^2$ in (6) is suppressed.

The exact equation for the pair correlation function $C(1;2)$ is still given by (11)

$$C(1;2) + \frac{1}{2} C(1;2) = \nabla^2 C(1;2) + F(1;2); \quad (30)$$

where, from (28) and (29), the NL term is now given by

$$F(1;2) = \frac{D}{2} T(1) \sim(1) \sim(2) \frac{E}{2}; \quad (31)$$

which must be replaced by some approximate non-linear function of $C(1;2)$ in order to transform (11) into a closed equation. Following the strategy of section 3, we introduce a non-linear mapping between the order parameter $\sim(\mathbf{r}; \sim)$, which is now not well defined near the defects, and an auxiliary 'smooth' field $\mathfrak{m}(\mathbf{r}; \sim)$. We can no longer define $\sim = \sim(\mathfrak{m})$ using the equilibrium profile equation of an isolated defect [14], which yields a trivial relation everywhere except at the defect cores where it is singular. The natural way to define the relation between the unit vector $\sim(\mathbf{r}; \sim)$ and $\mathfrak{m}(\mathbf{r}; \sim)$ amounts to replacing (13) by its discontinuous asymptotic form [22]

$$\sim(\mathfrak{m}) = \frac{\mathfrak{m}}{|\mathfrak{m}|} : \quad (32)$$

This mapping only determines $\mathfrak{m}(\mathbf{r}; \sim)$ up to a factor (which e.g., may be a function of time), and there is now no obvious physical interpretation for the new variable. Up to a factor, however, we may still regard $\mathfrak{m}(\mathbf{r}; \sim)$ as a position vector (close enough to a defect) like in section 3.

For mathematical convenience we assume that $\mathfrak{m}(\mathbf{r}; \sim)$ is a gaussian random field (with zero mean) at all times, described by the pair distribution function (14)–(15). All the averages over the ensemble of initial \sim configurations are replaced by gaussian averages on \mathfrak{m} , and can be evaluated as functions of $n, S_0(1), S_0(2)$, and $\mathbf{r}; \sim$, the normalized \mathfrak{m} -correlator, which contains all the dynamic dependence.

In the same spirit which lead to expression (18) in section 3, using the mapping (32) and the gaussian property of \mathfrak{m} we can show [23] that the NL term (31) is then given, as an approximate non-linear function of $C(1;2)$, by

$$F(1;2) = \frac{nD}{2} \frac{E}{|\mathfrak{m}(1)|^2} \frac{D}{(\mathfrak{m}(1))^2} \frac{E}{2} \frac{\partial C}{\partial S_0(1)} + S_0(1)^2 \frac{1}{3} \frac{\partial^2 C}{\partial S_0(1)^2}$$

$$\begin{aligned}
& + \frac{n}{(C_0(1;2))^2} \left((r C_0(1;2))^2 \frac{1}{3} \frac{\partial^2 C}{\partial C_0(1;2)^2} \right) \\
& + S_0(1) C_0(1;2) \frac{1}{3} \left(\frac{2n}{n-1} \frac{\partial^2 C}{\partial S_0(1) \partial C_0(1;2)} + Q_n(1;2) \right) \quad (33)
\end{aligned}$$

$$Q_n(1;2) = (n-3)(n-1) \frac{j_n(1) j_n(2)}{j_n(1) j_n(2)} \quad (34)$$

$$= \frac{1}{S_0(1) S_0(1) S_0(2)} \frac{(n-1) B_{\frac{n-1}{2}; \frac{1}{2}}}{2} F\left(\frac{1}{2}; \frac{3}{2}; \frac{n}{2}; (1;2)^2\right) \quad (35)$$

Using (15), (16) and (20) the NL term (33) can be fully expressed in terms of C_0 and S_0 . For example, the correlators $h_m(1)^2 i = C_0(1;2)_{2!-1}$ and $h(r m(1))^2 i = r^2 C_0(1;2)_{2!-1}$, the derivative $\partial C = \partial S_0(1) = C = 2S_0(1)$, where $C(\cdot) = \partial C = \partial$, and similarly for the other derivatives of $C(1;2)$. Substituting the NL term and the BPT function (20) into (30) we get the equation for $(1;2)$, which is the independent variable. Specializing to equal times ($t_1 = t_2 = t$), and looking for an isotropic scaling solution $(r; \cdot) = (x)$, we then obtain an approximate closed equation for (x) , the NLSM version of (22), the boundary conditions for which have been given in section 3. Even if we take S_0 to be time independent, this equation will still be much more complicated than (22).

If m in the NLSM is set to have the same interpretation as in section 3, and thus to obey (17), we may compare the NL terms (33) and (18). The NLSM gaussian approach generates the 'soft' field result, as long as $h(r m)^2 i = 1$, plus additional terms following from the consistent use of the mapping (32). This difference indicates that the gaussian approach is not quantitatively accurate, since (6) and (28) should yield equivalent asymptotic dynamics.

V. LINEAR-GAUSSIAN APPROXIMATION

Rather than solving the extremely complicated approximate non-linear equation for $(1;2)$, we propose a fully analytical scheme — the 'Linear-Gaussian' (LG) approach — to evaluate $C(1;2)$, which combines a gaussian mapping for a unit vector \tilde{m} with the large- n exact solution.

We notice that the relation $C = C(\cdot; n)$, defined by (19) and given by the BPT function (20) for a gaussian m , accounts effectively for the presence of the field defects (through the orientation of $\tilde{m} = j_n j_n$), and also for their topological nature (through the n -dependence), and so it already describes fairly well the late-time defect structure. Hence, the particular form of the function $(1;2)$, which contains the dynamical dependence of $C(1;2)$, should not be so relevant and may be approximated rather crudely. For simplicity, we replace \tilde{m} by \tilde{m}_1 , the exact

solution in the large- n limit [25]. The scaling function $f_{LG}(x_s; q) = C(1; 2)_{LG}$ with $n = 1; \dots; 4; 1$ and $\nu = 2$ and 4, obtained using this procedure, is plotted in figures 1 and 2 with fixed values of $q = q_2 = 1$ and abscissa $x_s = 2r = (r_1 + r_2)$, and in figures 3 and 4 with fixed values of x_s and abscissa q . More details are given in section 7 and in the figure captions.

As $n \rightarrow 1$, $\tilde{m} = (\tilde{m}_i^2)^{1/2} \rightarrow \sqrt{P/n S_0}$, and it is easy to find the limit of the functions Q_n and $C(\cdot)$, either from their definitions (34) and (19) or from their gaussian averages (35) and (20). The BPT function reduces to $C(\cdot; n) \rightarrow C_1$ and $Q_n(1; 2) \rightarrow 1 = S_0(1) = S_0(1)S_0(2)$. Equations (30)–(31) yield the self-consistent linear equation

$$f_1(1; 2) + \frac{1}{n} f_1(1; 2) = r^2 f_1(1; 2) + hT(1) f_1(1; 2); \quad (36)$$

$$hT(1) = T_0 = \frac{2}{n}; \quad (37)$$

where the scaling form (37) follows from a dimensional analysis of (36) or (29) (and from translational invariance), and the constant T_0 is to be found self-consistently (see (63) in the appendix). The linear term $F_1(1; 2) = hT(1) f_1(1; 2)$ is the limit of the previous NL term: the gaussian expression (33), or the definition (31) and (29), where $\tilde{m} \rightarrow \sqrt{P/n S_0}$.

Instead of determining $f_1(1; 2)$ by solving the linear equation (36) at equal times, which (like (21)) is third order, it is easier to calculate the correlation function of the exact large- n solution of the NLSM equation (28), which is second order. Equation (36) for $f_1 = C_1$ can be derived from the large- n limit of (28) (just like (30) was derived from (28)), so the two procedures to obtain f_1 are equivalent. Turok and Spergel [9] have solved the large- n NLSM in momentum space and determined the structure factor corresponding to a random initial field. In the appendix we present and Fourier-transform their result to 3-dimensional real space, yielding the scaling function $f_1(x; q) = C_1(r; 1; 2) = f_1(r; 1; 2)$:

$$f_1(x; q) = \frac{(1 + q - x)}{N} \frac{1}{x q^{1/2}} \int_A^{Z_B} ds s (1 - s^2)^{-1/2} (q^2 - (x - s^2)^{+1/2}); \quad (38)$$

where

$$x = r = r_1; \quad q = q_2 = 1; \quad (39)$$

$$\begin{aligned} (B; A) &= (x + q; x - q); \quad x = 1 - q \\ &= (1; x - q); \quad \int_1^q q^j x^{1+q} \\ &= (1; 1); \quad x = q = 1; \end{aligned} \quad (40)$$

and $N = 4=5; 32=63$ for $\nu = 2; 4$. At equal times,

$$f_1(x; 1) = \frac{(2 - x)}{N} \frac{1}{x} \int_{x-1}^{Z_1} ds s (1 - s^2)^{-1/2} (1 - (x - s^2)^{+1/2}); \quad (41)$$

The small- x behaviour of $f_1(x;1)$ can either be obtained from the large- n limit of the gaussian equation for τ , e.g. (22), or by expanding (41) as $x \rightarrow 0$. Both procedures yield the leading behaviour as $x \rightarrow 0$

$$\begin{aligned} f_1(x;1) &= 1 - (5/8) \ln(1-x) x^2 + \dots = 2 \\ &= 1 - (27/16) x^2 + \dots = 4; \end{aligned} \quad (42)$$

Expanding the BPT function (20) as $\tau \rightarrow 1$ and using (42) yields the small- x expansion for the equal-times pair correlation function within the LG approach. For a scalar field we have

$$\begin{aligned} f_{LG}(x;1) &= 1 - \frac{1}{5} \ln(1-x) x + \dots = 2; \quad n=1 \\ &= 1 - \frac{1}{27} x + \dots = 4; \quad n=1; \end{aligned} \quad (43)$$

and for a vector field

$$\begin{aligned} f_{LG}(x;1) &= 1 - A_1(x) x^2 + \dots = 2; \quad n > 1 \\ &= 1 - A_2 x^2 + \dots = 4; \quad n > 1; \end{aligned} \quad (44)$$

where $A_1(x) = (5/8) (\ln(1-x))^2$ and $A_2 = (27/16) \ln(1-x)$ for $n=2$, and $A_1(x) = (5/4) \ln(1-x)$ and $A_2 = 27/8$ for $n=3$. Performing a small- $(1+q-x)$ expansion of (38) we find the leading power-law decay

$$f(x;q) \sim f_1(x;q) \sim \frac{B(-\frac{q+1}{2}; \frac{1}{2})}{4(q+1)B(-\frac{q}{2}; 3/2)} \frac{q^{q+1}}{q^{q+2}} (1+q-x)^{q+1}; \quad (x \rightarrow 0); \quad (45)$$

In the limit of very-different times ($\tau_1 \rightarrow \tau_2$), we obtain the leading time-decay

$$f(x;q) \sim f_1(x;q) \sim \frac{1}{q^{3/2}} \frac{B(-\frac{q+1}{2}; 3/2)}{B(-\frac{q}{2}; 3/2)} + O(1/q^{7/2}); \quad (q \rightarrow 1); \quad (46)$$

By the same arguments discussed in section 3, the asymptotic forms (46) and (45) (the different-times generalization of (26)) are exact and the same for all n . In fact, as $x \rightarrow 1+q$ or $q \rightarrow 1$ and $\tau \rightarrow 0$ equation (30) becomes the linear equation (36), from which the same powers, but not the amplitudes, can be obtained.

VII. OTHER SCALING FUNCTIONS IN THE LG APPROACH

The LG method, implemented in section 5 to evaluate the pair correlation function, can be extended to other scaling functions. In this section we evaluate the pressure, the average energy density and the energy density correlation function.

As long as we replace \tilde{m} by its saturation form $m = jn$ (or $m = jn$ for a scalar field), the scaling functions will have built in the late-time defect structure.

Treating \mathbf{m} as a gaussian field, the dynamical dependence of the scaling functions is again embodied by $\langle \mathbf{r}; 1; 2 \rangle$. In the same spirit as in section 5, we replace by its large- n limit. In short, we keep in the n -dependence of the scaling properties through the gaussian averages over the \mathbf{m} vectors, and treat the gaussian moments of \mathbf{m} in the large- n limit. As mentioned in section 4, the mapping (32) only determines \mathbf{m} up to a factor (which may be time-dependent), and thus there is some freedom to fix the form of the second moment $S_0 = \langle \mathbf{m}^2 \rangle$. Although the choice $S_0 = \text{const}$ would greatly simplify the algebra (e.g. reducing the number of pair contractions of gaussian averages containing $\tilde{\mathbf{m}}$), we find it physically more convenient to regard \mathbf{m} as a length (close to a defect), and thus to keep the scaling form (17), i.e. $S_0 = 2^{-2} = \frac{1}{4}$. When written in terms of $\tilde{\mathbf{m}}$, though, the results are independent of the choice made.

The Higgs field energy density (see (7)) and isotropically averaged pressure are given by [5]

$$\langle \mathcal{E} \rangle = \frac{1}{2a(\tilde{\mathbf{m}})^2} \langle \tilde{\mathbf{m}}^2 \rangle^* + \langle \mathbf{r} \tilde{\mathbf{m}}^2 \rangle^+ + \langle D V(\tilde{\mathbf{m}}) \rangle^E \quad (47)$$

$$p(\tilde{\mathbf{m}}) = \frac{1}{2a(\tilde{\mathbf{m}})^2} \langle \tilde{\mathbf{m}}^2 \rangle^* - \frac{1}{3} \langle \mathbf{r} \tilde{\mathbf{m}}^2 \rangle^+ + \langle D V(\tilde{\mathbf{m}}) \rangle^E; \quad (48)$$

and scale as $1/t^2$, like the background \mathcal{E} and p . To evaluate \mathcal{E} and p within the LG approach, we first consider a vector field. In this case, the potential term is negligible (and identically zero in the NLSM) and can be ignored. Writing the derivatives of $\tilde{\mathbf{m}}$ in terms of the derivatives of \mathbf{m} , expanding the gaussian average into a sum of pair contractions, expressing the averages containing $\mathbf{r}_m \tilde{\mathbf{m}}$ as the limit $2!^{-1}$ of derivatives of $C(1;2)$ with respect to the gaussian moments, and treating \mathbf{m} in the limit $n!^{-1}$, yields

$$\langle \tilde{\mathbf{m}}^2 \rangle^* = C(1;1) \frac{\langle \mathbf{m}^2 \rangle}{S_0} = \frac{S_0}{2S_0} \langle \mathbf{m}^2 \rangle = C(1;1) \langle \mathbf{m}^2 \rangle^+ \quad (49)$$

$$\langle \mathbf{r} \tilde{\mathbf{m}}^2 \rangle^+ = C(1;1) \frac{\langle \mathbf{r}_m \mathbf{m}^2 \rangle}{S_0} = C(1;1) \langle \mathbf{r} \mathbf{m}^2 \rangle^+; \quad (50)$$

where $C(1;1) = \langle C(1;2) \rangle_{2!^{-1}} = (n-1)/(n-2)$ for $n \geq 3$, $C(1;1) = \ln(L=w)$ to leading order for $n = 2$ (where w is the string size, introduced as a short-distance cut-off), and

$$\begin{aligned} \langle \tilde{\mathbf{m}}^2 \rangle^* &= \langle \mathbf{m}^2 \rangle_{2!^{-1}} = \langle \mathbf{m}^2 \rangle_{1!^{-1}} = \frac{T_0}{(2)^{1/2}}; \\ \langle (\mathbf{r} \tilde{\mathbf{m}})^2 \rangle^E &= \langle (\mathbf{r}_1 \mathbf{r}_{2-1} \mathbf{m}^2) \rangle_{2!^{-1}} = \langle \mathbf{r}^2 \mathbf{m}^2 \rangle_{1!^{-1}} = \langle \mathbf{r}^2 \rangle_{1!^{-1}} \langle \mathbf{m}^2 \rangle^+; \end{aligned} \quad (51)$$

where we used (77) and $C_1 = 1$. Hence, from (47)–(50), the LG approach gives

$$\langle \mathcal{E} \rangle = \frac{n}{n-2} \langle \mathcal{E} \rangle_1; \quad p(\tilde{\mathbf{m}}) = \frac{n}{n-2} p_1(\tilde{\mathbf{m}}); \quad n > 2; \quad (52)$$

$$(\) = \ln(L=w) \quad ; \quad p(\) = \ln(L=w) \quad ; \quad n = 2 ; \quad (53)$$

with

$$_1(\) = \frac{T_0}{2} \frac{1}{a^2} \quad ; \quad p_1(\) = \frac{(4) T_0}{6} \frac{1}{a^2} : \quad (54)$$

In the radiation dominated era, where $\ = 2$, $_1(1;1)$ and $r^2 _1(1;1)$ (and $_1$ and p_1) have a leading order logarithmic divergence. Their difference, though, is finite and gives $hT_i = T_0 = 2$ (see (77)) (and also $p_1 = _1 = 1=3$). The relevant case, however, is the matter dominated era ($\ = 4$), when matter perturbations started to grow, yielding $p(\) = 0$ with $n = 2$ and

$$(\) = 6.75 + \frac{6.75}{n-2} \frac{1}{a^2} \quad ; \quad n > 2 : \quad (55)$$

Although a consistent implementation of the LG method requires the use of the NLSE, and thus a vector field, the approach can be extrapolated for a scalar field in an elegant manner. This was already done in section 5, where we simply extended the results for the scalar field correlation function taking $n = 1$ in the BPT function (see (43)), rather than deriving an equation for $C(1;2)$. The difference for a scalar field is that the wall width, w , plays a role in the dynamics, making the scaling functions (which contain time-dependent prefactors) differ from their dimensional analysis form. Moreover, the potential term in (47)–(48) has now a relevant contribution $hV_i = r^2 \sim 2a^2$. A convenient definition for the non-comoving wall width (which is constant in time for sharp domain walls) is $w = 4\sigma$, where σ is the non-comoving (or physical) surface tension given by

$$a(\) = \int_{-1}^1 dx (d_w = dx)^2 ; \quad (56)$$

where here $d_w(x)$ represents a single planar domain wall, and x is a comoving coordinate normal to the wall. The value of σ depends, through $d_w(x)$, on the explicit form of the driving potential. In the spirit of the LG approach we exploit the asymptotic mapping $\phi(m) = \text{sign}(m)$ to perform the gaussian averages, and treat the m -correlators in the large- n limit. To evaluate p and h , we write the derivatives of ϕ in terms of the derivatives of m and expand the gaussian average into a sum of pair contractions. Noting that $d = dm$ is sharply peaked at $m = 0$ and that $\int_{-\infty}^{\infty} dm \delta(m) = 1$, we get $h^{(2)}_i = \int_{-\infty}^{\infty} dm P(m) \phi^2 = a P(0)$, where $P(m) = e^{m^2 - 2S_0} = \frac{1}{\sqrt{2S_0}}$ is the one-point probability distribution form m . Using $\phi^2 = a - \phi(m)$ (which follows from (56)) and integrating by parts, we get $h^{(2)}_i = a h^{(0)}_i = a P^{(0)}(0)$. Therefore, $h^{(2)}_i = a \frac{1}{\sqrt{2S_0}} (1;1)$ and $h(r^2)_i = a \frac{1}{\sqrt{2S_0}} (r^2(1;1))$, which are the analogues of (49)–(50). Since ϕ embodies the extra physical feature of the scalar field, we can treat the remaining factors in the large- n limit. Taking $S_0 = 2 = T_0$

(which follows from (17) and (27)), $(1;1)! \sim \frac{1}{2} +$ and $r^2(1;1)! \sim (r \sim)^2 \frac{D}{1}$, which are then given by (77), we get, from (48)–(47),

$$(\) = \frac{2}{2 - T_0} \frac{1}{a} a_{-1}(\) ; p(\) = \frac{7}{2 - T_0} \frac{4}{3} a_{-1}(\) ; n = 1 : (57)$$

In the radiation dominated era ϵ and p have again a leading logarithmic divergence. In the matter dominated era, we obtain

$$(\) = \frac{7^{p \frac{6.75}{4}}}{2} \frac{1}{a} ; p(\) = \frac{3^{p \frac{6.75}{4}}}{2} \frac{1}{a} ; n = 1 : (58)$$

We now look to evaluate the correlations between the energy density terms of the Higgs field, i.e. ϵ^2 and $(r \sim)^2$. For simplicity we shall restrict to the case of a scalar field. Writing the derivatives of ϕ in terms of the derivatives of m , expanding the gaussian average into a sum of pair contractions, replacing ϕ^2 by a $\phi(m)$, doing some gaussian integrals by parts, using (14)–(15), and treating the m -correlators in the large- n limit, we obtain (with $\langle X Y \rangle_c = \langle X Y \rangle - \langle X \rangle \langle Y \rangle$)

$$n \left(\langle \phi_{11}^2 \rangle_1 \langle \phi_{22}^2 \rangle_2 + \langle \phi^2 \rangle_1 \langle \phi^2 \rangle_2 \right) + \langle \phi_{11}^2 \rangle_2 + 2 \langle \phi_{12}^2 \rangle_1 = \frac{A}{(1 - \frac{2}{n})^{5=2}} ; (59)$$

$$\left(\langle \phi_{11}^2 \rangle_r \langle \phi_{22}^2 \rangle_r + \langle \phi^2 \rangle_r^2 \right) + \langle \phi_{11}^2 \rangle_r + 2 \langle \phi_{rr}^2 \rangle_r + \frac{2}{r^2} \langle \phi^2 \rangle_r = \frac{A}{(1 - \frac{2}{n})^{5=2}} ; (60)$$

where $A = \frac{2}{n} a_{-1} a_{-2} (2 - T_0)$, $(1 - \frac{2}{n})$, and $\phi_{11} = \phi_{11}(1;2)$, $\phi_{12} = \phi_{12}(1;2)$, $\phi_r = \phi_{11} = \phi_r$, $\phi_{rr} = \phi_{11}^2 = \phi_r^2$, and $\phi_{11} = \phi_{11}(1;1)$, $\phi_{11} = r^2 \phi_{11}(1;1)$, are given by (75) and (77). We have checked that, as expected, the results are independent of whether we take S_0 to be constant or given by (17). The scaling functions corresponding to (59) and (60), normalized in the form $\langle X Y \rangle_c = \langle X \rangle \langle Y \rangle$, have been plotted in figures 5 and 6, respectively, for the matter era. Details and comments are given in the next section and in the figure captions.

VII. SUMMARY AND DISCUSSION

Two distinct gaussian approaches for the $O(n)$ Higgs field dynamics, in a flat expanding universe, were proposed to evaluate the pair correlation function, and other scaling functions. Both theories are based on a non-linear mapping between the order parameter $\phi(r; \epsilon)$ and an auxiliary field $m(r; \epsilon)$, which varies smoothly in the

vicinity of the eld defects. For simplicity and mathematical convenience, $\mathbf{r}(\mathbf{r}; \cdot)$ is assumed to be a gaussian random eld, yielding an approximate closed scheme to evaluate the scaling functions. The eld $\tilde{\phi}$ itself, which is effectively discontinuous near the defects, is not suitable to be treated as gaussian.

In the 'soft' eld theory of section 3, based on the equation of motion (6), we have followed Mazenko's gaussian approach [14, 16] for model A dynamics, where the mapping is defined by the equilibrium profile equation $\mathbf{r}_m^2 \tilde{\phi} = \partial V / \partial \tilde{\phi}$. In this case, $\mathbf{r}(\mathbf{r}; \cdot)$ is identified as a position vector relative to the nearest eld defect. The mapping (13), however, is incompatible with the late-time eld oscillations in the bulk (10) (which are absent in purely relaxational systems). By studying the linear dynamics of the gaussian moment $C_0(1;2)$, given by equation (15), we can prove that this theory is inconsistent, and therefore we have not looked to solve numerically the rather complicated equations (22) or (23). The fact that, despite this intrinsic inconsistency, the pair correlation function displays correct physical features, such as (24) and (26), is not, however, a merit of the approximation used. The small- x Porod's regime for a scalar eld follows from the use of the BPT function (20), which has built in the late-time defect structure, and the asymptotic power-decay, which occurs in the linear (small- $f(x)$) regime, is universal for all $O(n)$ 'soft' and 'hard' eld models.

In section 4, we have developed a more consistent theory, based on the NLSM, or 'hard' eld, dynamics (28). We do not expect the eld bulk oscillations (10) to have a relevant effect on the scaling properties, so we consistently fix the eld magnitude to eliminate the previous mapping incompatibility. Also, since the eld now evolves on the vacuum manifold, the dynamics are independent of the driving potential. The auxiliary eld is now defined by $\tilde{\phi}(\mathbf{r}) = \mathbf{r} = \mathbf{j} \cdot \mathbf{r}$. Although it can still have the same interpretation as in section 3, \mathbf{r} is only determined up to a factor and we are free to choose $\langle \mathbf{r}^2 \rangle = 1$. The relation $C(\cdot; n)$, between the pair correlation function and the normalized \mathbf{r} -correlator, is given by the BPT function (20) for a gaussian \mathbf{r} , and $\tilde{\phi}$ obeys an approximate equation, derivable from (30)–(33).

Rather than solving this complicated equation for $\tilde{\phi}$, in section 5 we propose a fully analytical scheme to evaluate $C(1;2)$. Recognizing that the BPT function captures the essential late-time defect structure, we approximate the asymptotic eld dynamics even further replacing $\tilde{\phi}$ by ϕ_1 , the exact solution for the limit $n \rightarrow 1$. The pair correlation function is then given (in a symbolic notation) by $C(1;2)_{LG} = BPT(\phi_1(1;2); n)$. Although the NLSM only holds for vector elds, the LG approach can be extended to $n = 1$, since it only depends on the large- n dynamics, which is the same for both equations (6) and (28). In this case the scaling properties are evaluated using the mapping $\phi(\mathbf{r}) = \text{sign}(\mathbf{r} \cdot \mathbf{r})$ and the gaussian

assumption. The pair correlation function, for instance, is again given by the BPT function, with $n = 1$, and by the same argument we replace β by β_1 . The scaling form $f_{LG}(x; q)$, for $n = 1; \dots; 4; 1$ and in the radiation and matter dominated eras, is plotted in: figures 1 and 2, respectively, with different fixed values of q and abscissa $x_s = 2r = (r_1 + r_2) = 2x = (1 + q)$, and in figures 3 and 4, respectively, with different fixed values of x_s and abscissa q . The normalization is as follows: $f(0; 1) = 1$ for $q = 1$; for $q \neq 1$ we used the time-dependent condition $f(x; q) = \beta_1(x; q) / \beta_1(0; 1)$ as $x \rightarrow 0$, such that curves with different n cut the origin at the same point.

The LG approach for the Higgs model is the analogue of the Ohta-Jasnow-Kawasaki approximate scheme in model A dynamics [12]. In that case, $f_1(x; 1) = \exp(-x^2/8)$. The greater complexity of (38)–(41) is due to the causal condition (9) which these obey. The main physical features are preserved in this approach: the threshold power-law behaviour (45) (imposed by causality) is exact, and for $n = 1$ a linear Porod's regime, (43), is obtained for $\beta = 4$. For $\beta = 2$, however, we obtain a logarithmic modified Porod's regime, $f(x; 1) = 1 + O(x \ln x)$ (slightly apparent in figure 1), which is probably an artifact of the LG approach and has no physical meaning. This logarithmic correction is absent in the small- x expansion (24) of section 3.

We have seen in section 5 that all the exact and the gaussian expressions have the same limit as $n \rightarrow 1$. In fact, the gaussian approach becomes exact (for random gaussian initial conditions) in this limit since the equation for \tilde{m} becomes linear. This equation is derived from the linearised equation for \tilde{m} (replacing \tilde{m} by $\tilde{m} = \frac{p}{n} S_0$), and its form depends on the choice made for S_0 . Also, the two gaussian approaches, for the 'soft' field and for the NLSM, become equivalent (and exact) as $n \rightarrow 1$ and the LG approach could be implemented equally well using either. We end, however, that the NLSM provides a more systematic and self-consistent framework for this purpose, while the 'soft' field model yields the physical motivation to employ the NLSM (and proves useful in the LG calculation of other scaling functions with $n = 1$).

In section 6 we have extended the LG approach to evaluate other scaling properties of the Higgs field. For these cases we do not know how to build closed approximate equations like those of sections 3 and 4, and the method proves especially useful. If we restricted ourselves to the gaussian approach we could express other scaling functions in terms of \tilde{m} and its derivatives, but we could not solve for these derivatives numerically. For a scalar field we can still use the asymptotic mapping $(\tilde{m}) = \tilde{m} = j n j$, but we have to account for the non-trivial role of the wall width, w , which is inversely proportional to β , the surface tension (56). The LG results (52), (53), (57), give the average field energy density (47) and pressure (48) as being

proportional to ρ_1 , the energy density in the limit $n \rightarrow 1$. The factor of proportionality is n -dependent, and is also time-dependent for $n = 2$ and $n = 1$. Since ρ_1 and p_1 , given by (54), have a leading logarithmic divergence at $\tau = 2$, we have discarded the radiation dominated era, which is a less relevant case in the formation of cosmic structure, and next summarize the LG results in the matter era ($\tau = 4$). With $n > 2$, (55) gives $\rho = 6.75(1 + 1/(n-2))a^2$, which compared with the τ to simulation results [11]: $6.75(1 + (20/9)/(n-2))a^2$ shows a fair agreement up to a factor 2 in the correction term. With $n = 1$, (58) gives $\rho = \text{const} = a$, yielding energy density fluctuations growing linearly with time, rather than having a constant value as in the vector case. This well known result [5] means that walls, if present, would rapidly dominate the energy of the universe. With $n = 2$ we obtain zero pressure, as expected. With $n = 1$ we get a negative pressure $p = -3/7$, yielding a source term $\rho + 3p < 0$, which can be regarded as indicating an effective domain wall repulsion [5] in the scaling regime, and is a reflection of domain growth. We recall that for an isolated equilibrium domain-wall perpendicular to the x direction (for which $\partial^2 = 0 = \partial/\partial y = \partial/\partial z$), the field pressure components along each axis are $p_x = 0$ and $p_y = p_z = -\rho/2$ [5]. The pole of (52) at $n = 2$ is built in the approach through the use of a unit vector (i.e. the defect core-size $w \neq 0$) since, in fact, the ‘sharpness’ of the string cores leads to a logarithmic cut-off given in (53) [26].

Finally, we have done a LG calculation of the correlations between the energy terms ρ^2 and $(\rho \sim)^2$, which are the sources for the perturbations in the cosmological matter distribution. For simplicity we have restricted ourselves to the case of a scalar field. In contrast to the vector case, ρ^2 cannot be regarded as the ‘centripetal’ energy due to the field wandering around in the ‘vacuum manifold’. At late-times, though, ρ^2 , or $(\rho \sim)^2$, vanish everywhere in the bulk regions and thus probe the presence of domain walls (where energy is concentrated). Using (38) and (77), we have computed the scaling function $-\langle \rho^2(1)^2 \rho^2(2)^2 \rangle_c = -\langle \rho^2(1)^2 \rho^2(2)^2 \rangle$, given by (59), in the matter era. Figure 5 shows the results with different fixed values of $q = \tau_2/\tau_1$ and abscissa $x_s = 2x/(1+q)$. Remarkably, as x increases from zero there is a dramatic change from large positive values to negative values. We interpret these set of plots as giving evidence of domain walls dynamics (in a statistical sense): the correlation peak (for fixed q) is displaced along the ‘distance’ axis as the time separation between the two points increases (i.e. as q departs from 1). Its amplitude decrease is dictated by statistical incoherence as the points move apart, and its displacement, $x_{s,\text{peak}}$, must be proportional to the typical distance traveled by a wall during the time $t_{D,E}^{1/2}$. The equal-time ($q = 1$) divergence of the peak at the origin (i.e. of ρ^4) is an artifact of the absence of a short-distance cut-off in $\rho_1(x;1)$ as r drops below the

wall width w . The scaling function $h(r_1)^2(r_2)^2 i_c = h(r_1)^2 i h(r_2)^2 i$, given by (60), is plotted in figure 6 for the matter era. In this case the peak remains at the origin, while its amplitude decreases, as q departs from 1. Since both energy density terms probe the presence of domain walls, it is not very clear to us why this correlation function is so different from the previous one shown in figure 5. It seems that its form for $x < 0.5$ is entirely dictated by its singular prefactor $1 = (1 - \frac{2}{1})^{5/2}$, which is plotted in figure 7.

We conclude by discussing some directions for future work. By linearizing the full equation of motion (11), with (18) or (33), for the correlation function around the scaling solution, it should be possible to show that the scaling solution is a stable attractor of the dynamics. In particular, the prescaling regime (e.g. corrections to scaling) can be described using the gaussian closure schemes of sections 3 or 4. The early-time behaviour, however, is not accessible within the auxiliary field methods utilized here, which assume a well-defined defect structure. The dependence on the initial state of the system before the phase transition is also of interest. In the present work, short-range spatial correlations in the initial state are considered, appropriate for a disordered system in equilibrium at high temperature. In the context of model A dynamics, it has been shown that the asymptotic scaling behavior is modified if sufficiently long-ranged power-law correlations are present in the initial state [27]. Such correlations can also be incorporated in the LG approach, through a modification of the large- n solution presented in the appendix. Finally, the extension of the functions (59) and (60) for vector fields, which involves extensive calculations, can be used to evaluate the correlations between the matter distribution perturbations induced by the Higgs field [11] and may, therefore, have a direct cosmological interest.

ACKNOWLEDGEMENTS

We thank N. Turok for many helpful discussions and suggestions, and M. Birse for comments on the manuscript. J.F. thanks JNICT (Portugal) for a research studentship.

APPENDIX : the large- n solution of the NLSM

For simplicity we shall still take $\tilde{\omega}^2 = 1$, which differs from the usual normalization, $\tilde{\omega}^2 = n$, used to solve large- n models.

To leading order as $n \rightarrow 1$ the NL factor (29) is replaced by its average (over initial conditions), $T(r; \omega) \rightarrow \overline{hT(r; \omega)}$, which one expects to have the scaling form (37), i.e. $\overline{hT(r; \omega)} = T_0 \omega^{-2}$, where T_0 is a constant to be determined self-consistently. The equation of motion (28) becomes linear and has been solved in momentum space, with the following initial conditions, at some early time $\omega_0 > 0$ after the SSB

transition [9]: $\tilde{\epsilon}(\mathbf{r}; 0)$ is a (gaussian) random unit vector in each initial correlation volume e , i.e. its Fourier components are white noise correlated, $\tilde{\epsilon}_k(0) \tilde{\epsilon}_k(0) = \delta_{\mathbf{k}}; \langle \tilde{\epsilon}_k(0) \rangle = 0$ as $k \rightarrow 0$, to ensure that $\langle \tilde{\epsilon}(\mathbf{r}; 0) \rangle = 0$ respects the assumption of homogeneity of the early universe on scales above the horizon. The solution obtained is [9]

$$\tilde{\epsilon}_k(\mathbf{r}) = A \frac{J_3(kr)}{kr^3} \tilde{\epsilon}_k(0); \quad (61)$$

$$A = \frac{1}{2} \quad (62)$$

$$T_0 = \frac{3}{2} (2 + 1) = 4; \quad (63)$$

where $A = \frac{1}{2} (2 + 1)$ and $J(z)$ is a Bessel function of the first kind. The second linearly independent solution is ruled out since $Y(kr) \rightarrow \infty$ as $k \rightarrow 0$. From (61) one finds the structure factor

$$\langle \tilde{\epsilon}_k(\mathbf{r}_1) \tilde{\epsilon}_k(\mathbf{r}_2) \rangle = A^2 \frac{(kr_1)^3 (kr_2)^3}{(kr_1)^3 (kr_2)^3} J_3(kr_1) J_3(kr_2); \quad (64)$$

To obtain the pair correlation function we Fourier transform (64). Using the normalization $C_1(0; \mathbf{r}_1, \mathbf{r}_2) = 1$, we have

$$\begin{aligned} C_1(\mathbf{r}; \mathbf{r}_1, \mathbf{r}_2) &= \langle \tilde{\epsilon}(\mathbf{r}; 0) \tilde{\epsilon}(\mathbf{r}; 2) \rangle \\ &= \int \frac{d^3k}{(2\pi)^3} \tilde{\epsilon}_k(\mathbf{r}_1) \tilde{\epsilon}_k(\mathbf{r}_2) e^{i\mathbf{r} \cdot \mathbf{k}} = \int \frac{d^3k}{(2\pi)^3} \tilde{\epsilon}_k(\mathbf{r}_1) \tilde{\epsilon}_k(\mathbf{r}_1) \\ &= \frac{(kr_1)^3}{N_1} \int \frac{d^3k}{(2\pi)^3} \frac{J_3(kr_1) J_3(kr_2)}{(kr_1)^3 (kr_2)^3} e^{i\mathbf{r} \cdot \mathbf{k}} \end{aligned} \quad (65)$$

$$N_1 = \int \frac{d^3y}{y^3} \frac{J_3(y)}{y} = \frac{B(3/2)}{2^2} = \frac{1}{2} \quad (66)$$

Clearly, from (65), $C_1(\mathbf{r}; \mathbf{r}_1, \mathbf{r}_2)$ has the scaling form $f_1(\mathbf{x}; q)$, with $\mathbf{x} = \mathbf{r} - \mathbf{r}_1$ and $q = r_2 - r_1$. To evaluate (65) we write it in the convenient form

$$\begin{aligned} f_1(\mathbf{x}; q) &= \frac{q^3}{N_1} \int \frac{d^3y}{y^3} \frac{J_3(y) J_3(yq)}{y (yq)} e^{i\mathbf{x} \cdot \mathbf{y}} \\ &= \frac{2}{N_1} \frac{q^3}{x} \frac{1}{dx} \int_0^1 dy \cos(yx) \frac{J_3(y) J_3(yq)}{y (yq)}; \end{aligned} \quad (67)$$

Using the integral representation of Bessel functions [24], we have

$$\begin{aligned} I(\mathbf{x}; q) &= \frac{2}{(1+x)^2} \int_0^1 dy \cos(yx) \frac{J_3(y) J_3(yq)}{y (yq)} \\ &= \frac{2}{(1+x)^2} \int_0^1 dy \int_0^1 ds \int_0^1 dt (1-s)^2 (1-t)^2 \cos(yx) \cos(ys) \cos(yqt) \end{aligned}$$

$$\begin{aligned}
&= \frac{1}{(1+q)^{q+2}} \int_0^1 ds \int_0^1 dt (1-s)^{\frac{q+1}{2}} (q^2-t)^{\frac{q+1}{2}} f(x+s-t) + f(x-s+t) + f(x+s+t)g \\
&= \frac{1}{(1+q)^{q+2}} \int_1^Z ds (1-s)^{\frac{q+1}{2}} (q^2-(x-s)^2)^{\frac{q+1}{2}} (s+q-x)(q+x-s) \quad (68) \\
&= \frac{(1+q-x)}{(1+q)^{q+2}} \int_A^Z ds (1-s)^{\frac{q+1}{2}} (q^2-(x-s)^2)^{\frac{q+1}{2}} ; \quad (69)
\end{aligned}$$

alternatively, performing the 'self-similar' transform $s \rightarrow x-s$ in (68),

$$\begin{aligned}
I(x;q) &= \frac{1}{(1+q)^{q+2}} \int_{x-1}^{x+1} ds (1-(x-s)^2)^{\frac{q+1}{2}} (q^2-s^2)^{\frac{q+1}{2}} (q-s)(q+s) \\
&= \frac{(1+q-x)}{(1+q)^{q+2}} \int_{x-B}^{x+A} ds (1-(x-s)^2)^{\frac{q+1}{2}} (q^2-s^2)^{\frac{q+1}{2}} ; \quad (70)
\end{aligned}$$

$$\begin{aligned}
(B;A) &= (x+q;x-q) ; x-1-q \\
&= (1;x-q) ; 1-q ; x-1+q \\
&= (1;-1) ; x-q-1 ; \quad (71)
\end{aligned}$$

Differentiating $I(x;q)$ with respect to x we get, using some of the possible integral representations for $\partial I/\partial x$,

$$\begin{aligned}
f_1(x;q) &= \frac{q^{3=2}}{N(x)} \frac{\partial I(x;q)}{\partial x} \\
&= \frac{(1+q-x)}{N(x)q^{1=2}} \int_A^Z ds (x-s) (q^2-(x-s)^2)^{\frac{q+1}{2}} (1-s)^{\frac{q+1}{2}} \quad (72)
\end{aligned}$$

$$= \frac{(1+q-x)}{N(x)q^{1=2}} \int_A^Z ds s (1-s)^{\frac{q+1}{2}} (q^2-(x-s)^2)^{\frac{q+1}{2}} \quad (73)$$

$$= \frac{(1+q-x)}{N(x)q^{1=2}} \int_A^Z ds \frac{fs(q^2-1)+x(1-s(x-s))q}{2} (1-s)^{\frac{q+1}{2}} (q^2-(x-s)^2)^{\frac{q+1}{2}} \quad (74)$$

where $N = (q+1)B(q;3=2)$. Expression (72) follows from differentiating (69). The form (73), which follows from (70) and the transformation $s \rightarrow x-s$, or from integrating (72) by parts, is convenient for further differentiation with respect to x . Finally, (74) is the mean of the previous two, and proves useful at equal times ($q=1$) where the factor $1=x$ gets canceled and higher derivatives with respect to x become easier to evaluate.

By construction $I(x;q)$ must be invariant under interchange of times, i.e. $I(x;q) = I(x=q;1=q)$. Since it is not explicitly symmetric, a number of integration variable changes and other transformations may be performed in $I(x;q)$ and $dI(x;q)=dx$ leading to different equivalent integral representations for f_1 . However, the expressions given, with three different integration limits (71) depending on x and q , admit no further simplification. Writing the integrand in, say, (69), as $(x;q;s)^{\frac{q+1}{2}}$, it is easy to see that $(x;q;s) = (1-s)(1+s)(q+x-s)(q-x+s)$ is non-negative and

bounded only in the regions where both $|j| \leq 1$ and $x = q \pm s = x + q$, which are precisely those yield by (71). Hence, since $\frac{+1}{2}$ is non-integer, the integral (69) runs over the whole (bounded) region where the integrand is real. As illustrated by the small- x expansion (42), $I(x; q)$ is singular for $\nu = 2$. In fact, at each integration limit one (or two, if $x = 0$) of the radicals in $I(x; q; s)$ vanishes and high enough derivatives of the integrand or integration limits will diverge. Up to fourth order, however, we get finite derivatives of $I(x; q)$, but since each of the radicals in (69) can only be differentiated twice, one has to transform the integral, e.g. using $r \pm s \rightarrow \pm s$ (or integrating by parts) before doing the third and fourth derivatives. Using these methods we find, from (38), with $\nu = 2$,

$$\begin{aligned}
C_1(1; 2) &= \frac{1}{1} \frac{1}{N(x, q)} \int_A^{Z_B} ds F_{x;1} \quad C_1(1; 2) \\
C_1(1; 2) &= \frac{1}{2} \frac{1}{N(x, q)} \int_A^{Z_B} ds q F_{x;2} \quad C_1(1; 2) \\
C_1(1; 2) &= \frac{1}{1 \cdot 2} \frac{1}{N(x, q)} \int_A^{Z_B} ds q F_{x;1;2} \quad {}^2C_1(1; 2) \quad {}_1C_1(1; 2) + {}_2C_1(1; 2) \\
\frac{\partial C_1(1; 2)}{\partial r} &= \frac{1}{1} \frac{1}{N(x, q)} \int_A^{Z_B} ds F_{x^2} \quad \frac{C_1(1; 2)}{x} \\
r^2 C_1(1; 2) &= \frac{1}{\frac{2}{1}} \frac{1}{N(x, q)} \int_A^{Z_B} ds F_{x^3} \quad (75)
\end{aligned}$$

where it is implicit that $x = 1 + q$, and

$$\begin{aligned}
F_{x^2} &= (q^2 - (x - s^2))(1 - s^2)^{(+1)=2} (q^2 - (x - s^2))^{(-3)=2} \\
F_{x^3} &= (+1)s(q^2 - (x - s^2))(1 - s^2)^{(-1)=2} (q^2 - (x - s^2))^{(-3)=2} \\
F_{x;1} &= (+1)(x - s)(1 - s^2)^{(-1)=2} (q^2 - (x - s^2))^{(-1)=2} \\
F_{x;2} &= (-1)q(x - s)(1 - s^2)^{(+1)=2} (q^2 - (x - s^2))^{(-3)=2} \\
F_{x;1;2} &= (-2-1)q(x - s)(1 - s^2)^{(-1)=2} (q^2 - (x - s^2))^{(-3)=2} : \quad (76)
\end{aligned}$$

We also obtain in the limit $2 \rightarrow 1$, i.e. $r \rightarrow 0$ and $2 \rightarrow 1$,

$$\begin{aligned}
C_1(1; 1) &= 0 \quad ; \quad r C_1(1; 1) = 0 \\
C_1(1; 1) &= \frac{1}{\frac{2}{1}} \frac{T_0}{2} = r^2 C_1(1; 1) + \frac{T_0}{\frac{2}{1}} \\
r^2 C_1(1; 1) &= \frac{1}{\frac{2}{1}} \frac{T_0}{2} : \quad (77)
\end{aligned}$$

References

- [1] J.D. Gunton, M. San Miguel and P.S. Sahni in Phase transitions and Critical Phenomena, Vol. 8, C. Domb and J.L. Lebowitz (New York, Academic) (1983).
- [2] P.C. Hohenberg and B.I. Halperin, Rev. Mod. Phys. 49, 3 (1977).
- [3] K. Binder and D. Stauffer, Phys. Rev. Lett. 33, 1006 (1974); J. Marro, J.L. Lebowitz and M.H. Kalos, *ibid* 43, 282 (1979); H. Furukawa, Prog. Theor. Phys. 59, 1072 (1978); Phys. Rev. 43, 136 (1979).
- [4] S. Weinberg in Gravitation and Cosmology, Wiley-New York (1972).
- [5] A. Vilenkin, Phys. Rep. 121, 263 (1985); E.W. Kolb and M.S. Turner in The Early Universe, Addison-Wesley (1990).
- [6] T.W. Kibble, J. Phys. A 9, 1387 (1976).
- [7] A. Vilenkin, Phys. Rev. Lett. 46, 1169 (1981); Y.B. Zel'dovich, Mon. Not. R. Astron. Soc. 192, 663 (1980).
- [8] D.N. Spergel and N.G. Turok, Scient. Am. (March 1992).
- [9] N.G. Turok and D.N. Spergel, Phys. Rev. Lett. 66, 3093 (1991).
- [10] A. Albrecht and N. Turok, Phys. Rev. Lett. 54, 1868 (1985); D.P. Bennett and F.R. Bouchet, Phys. Rev. Lett. 60, 257 (1988); B. Allen and E.P.S. Shellard, Phys. Rev. Lett. 64, 119 (1990).
- [11] U.L. Pen, D.N. Spergel and N. Turok, Phys. Rev. D, 49, 692 (1994).
- [12] T. Ohta, D. Jasnow and K. Kawasaki, Phys. Rev. Lett. 49, 1223 (1982).
- [13] K. Kawasaki, M.C. Yalabik and J.D. Gunton, Phys. Rev. A 17, 445 (1978).
- [14] G.F. Mazenko, Phys. Rev. Lett. 63, 1605 (1989); Phys. Rev. B 42, 4487 (1990).
- [15] A.J. Bray and S. Puri, Phys. Rev. Lett. 67, 2670 (1991); H. Toyoki, Phys. Rev. B 45, 1965 (1992).
- [16] A.J. Bray and K. Humayun, J. Phys. A 25, 2191 (1992); F. Liu and G.F. Mazenko, Phys. Rev. B 45, 6989 (1992).
- [17] C. Yeung, Y. Ono and A. Shinozaki, Phys. Rev. E 49, 2693 (1994).
- [18] A.J. Bray and K. Humayun, Phys. Rev. E 48, R1609 (1993).
- [19] J.A.N. Filipe, unpublished.
- [20] G. Arfken in Mathematical Methods for Physicists, Academic Press (1985).

- [21] G .Porod in Sm allAngle X -ray Scattering, edited by O .G latter and O .K ratky, Academic-New York (1982).
- [22] W e thank N .Turok for this suggestion.
- [23] J.A .N .Filipe, unpublished.
- [24] Abram ow itz and Stegun in Handbook ofm athem atical functions, Dover.
- [25] This approach ism athem atically equivalent to the approxim ations used in references [12, 13, 15] for condensed m atter system s described by M odelA ' dynam ics.
- [26] e.g. see reference [5] and H .Toyoki, reference [15].
- [27] A .J.B ray, K .Hum ayun and T .J.N ewm an, Phys. Rev. B 43, 3699 (1991).

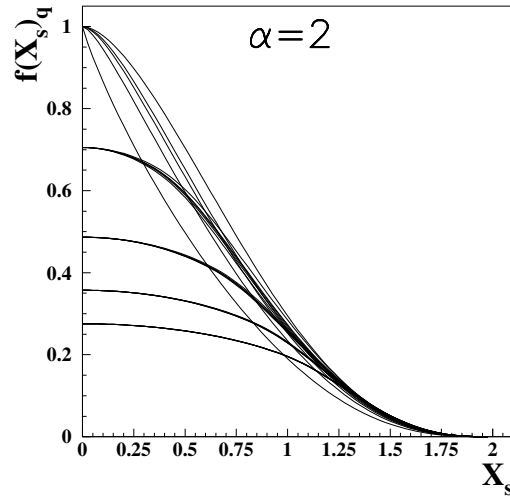


Figure 1: Field pair-correlation scaling function $C(1,2) = f(x,q)$ in the LG approach for the radiation dominated era (see (20) and (38)). Abscissa: $x_s = 2r/(\eta_1 + \eta_2)$. Each set of lines (crossing at $x = 0$) is a collapse of the plots for $n = 1, 2, 3, 4, \infty$ field components with a fixed ratio $q = \eta_2/\eta_1 = 1, 1.5, 2.0, 2.5, 3.0$ (bottom). Normalization: $f(x, 1) = 1$ for $q = 1$, and $f(x, q)/\gamma_\infty(x, q) \rightarrow 1$ as $x \rightarrow 0$ for all $q \neq 1$ and n , i.e. we have replaced (20) by $C(\gamma_\infty(x, q)) = \gamma_\infty(x, q) F(a, a; c; \gamma_\infty(x, q)^2)/F(a, a; c; \gamma_\infty(0, q)^2)$ ($a = 1/2, c = (n+1)/2$). This time-dependent condition assures that the point where each curve cuts the origin is the same for all n . In all plots $f(x, q) = 0$ for $r > \eta_1 + \eta_2$ (causality). The modified Porod's regime for $n = 1$: $f(x, 1) = 1 + O(x \ln(x))$ as $x \rightarrow 0$, is an artifact of using the large- n solution.

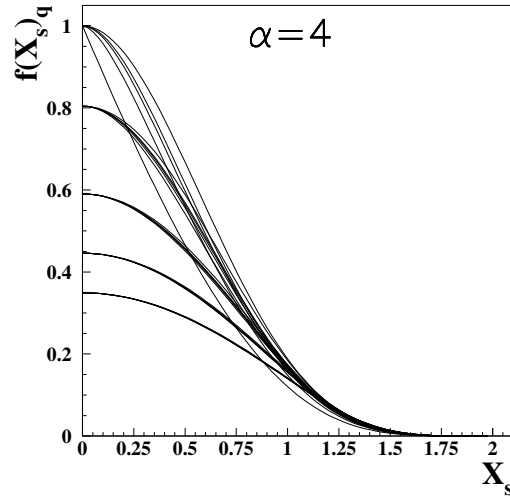


Figure 2: The same as in figure 1 but for the matter dominated era. We find the usual Porod's regime for $n = 1$: $f(x, 1) = 1 + O(x)$ as $x \rightarrow 0$ (see (43)).

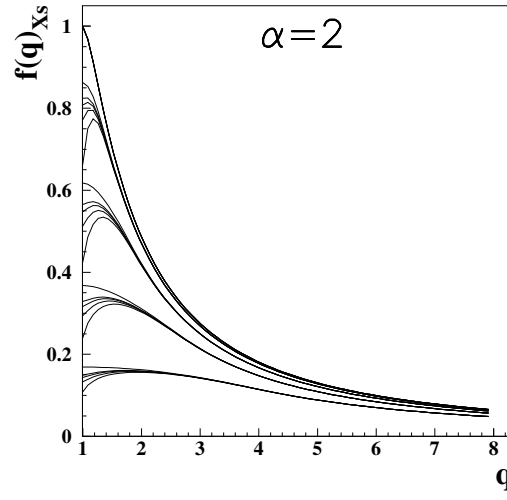


Figure 3: Field pair-correlation scaling function $C(1,2) = f(x,q)$ in the LG approach for the radiation dominated era (see (20) and (38)). Abscissa: $q = \eta_2/\eta_1$. Each set of lines (merging as $q \rightarrow \infty$) is a collapse of the plots for $n = 1, 2, 3, 4, \infty$ with a fixed $x_s \simeq 0.0, 0.3, 0.6, 0.9, 1.2$ (bottom). The top curve gives the time-decay at $x = 0$ in figure 1. All curves fall off like $1/q^{3/2}$ as $q \rightarrow \infty$ (see (46)), and are (by symmetry) invariant under the change $q \rightarrow 1/q$. The apparent singularity and correlation increase with q , between $q = 1$ and 2, is an artifact of the time-dependent normalization used in figures 1 and 2. Using a time-independent normalization, which is then n -dependent, we find that all curves are monotonically decreasing as q departs from 1, but curves with different values of x_s and n are difficult to distinguish.

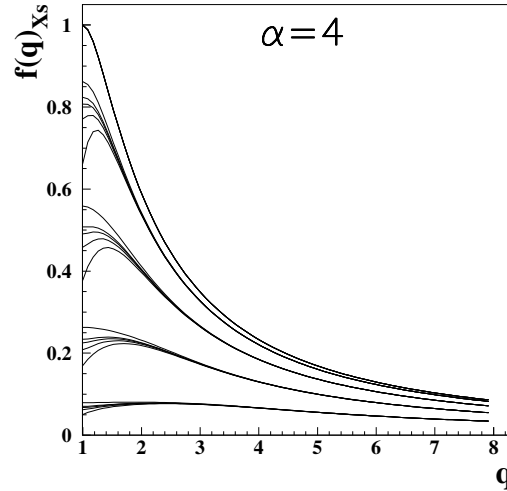


Figure 4: The same as in figure 3 but for the matter dominated era.

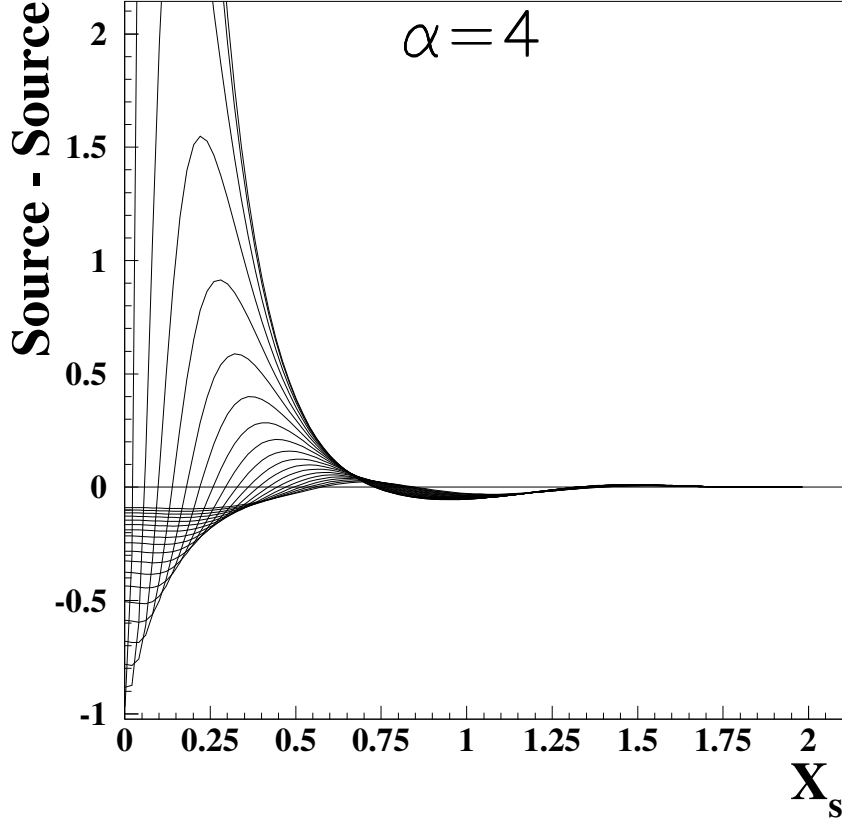


Figure 5: Source-source (energy density) pair-correlation scaling function $\langle \dot{\phi}^2(1)\dot{\phi}^2(2) \rangle_c / \langle \dot{\phi}^2(1) \rangle \langle \dot{\phi}^2(2) \rangle$ in the LG approach, given by (59), for a scalar field in the matter dominated era. Abscissa: $x_s = 2 r / (\eta_1 + \eta_2)$. Each plot is for a different fixed ratio $q = \eta_2 / \eta_1$: from $q = 1.0$ (top) to $q = 2.0$ (bottom), with steps $\Delta = 0.05$. There is interesting evidence of domain walls dynamics: the correlation peak (for fixed q) moves along the ‘distance’ axis as time-separation between the two points increases (i.e. as q departs from 1). The displacement should be proportional to the typical distance traveled by a wall during time $|\eta_2 - \eta_1|$. The peak amplitude decreases due to statistical incoherence as the points move apart. The equal-time ($q = 1$) divergence at the origin is an artifact from the assumption of ‘infinitely sharp’ walls ($w \rightarrow 0$).

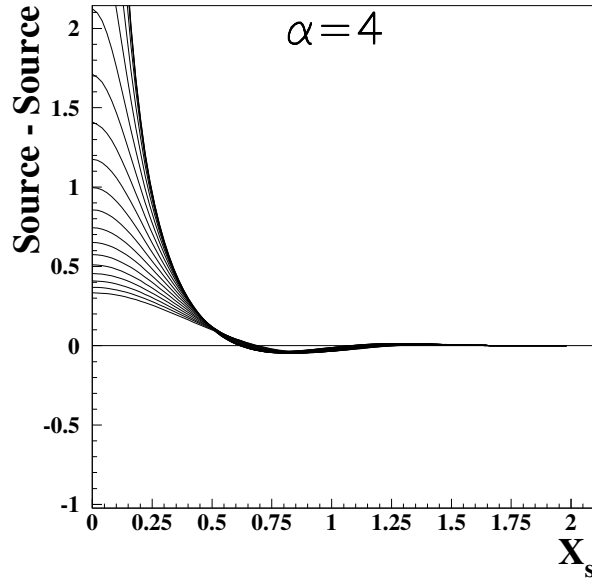


Figure 6: The source-source pair-correlation scaling function in the LG approach $\langle(\nabla\phi(1))^2(\nabla\phi(2))^2\rangle_c / \langle(\nabla\phi(1))^2\rangle\langle(\nabla\phi(2))^2\rangle$, given by (60), with the same specifications as in figure 5. In this case the correlation peak, while decreasing in amplitude, remains at the origin. Below $x = 0.5$ its form seems to be dictated by its singular prefactor, shown in figure 7.

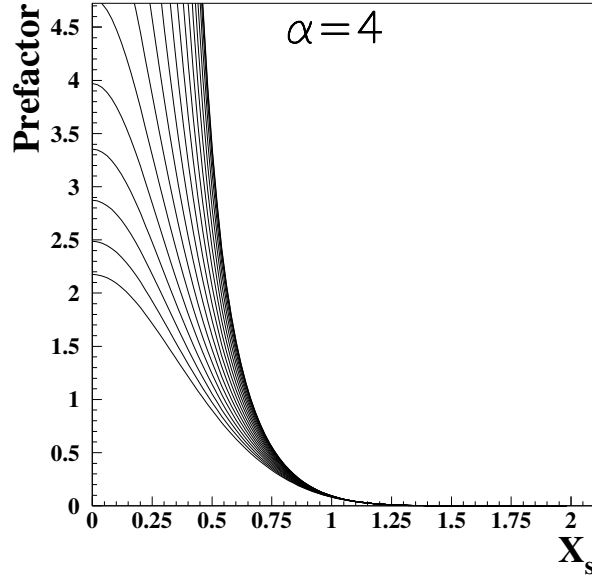


Figure 7: The prefactor $1/(1 - \gamma_\infty^2)^{5/2}$ in expressions (59) and (60), as a function of x and for fixed values of q in the same range as in figures 5 and 6.